Macromolecules

ARTICLE

pubs.acs.org/Macromolecules

Highly Site Specific, Protease Cleavable, Hydrophobic Peptide−Polymer Nanoparticles

Matthias Maier,[†] Niklas Kotman,[†] Cornelius Friedrichs,[†] Julien Andrieu,[†] Manfred Wagner,[†] Robert Graf,[†] Wolfgang S. L. Strauss,[‡] Volker Mailänder,[†,§] Clemens K. Weiss,[†] and Katharina Landfester*[,†]

[†]Max-Planck-Institute for Polymer Research, Ackermannweg 10, 55128 Mainz, Germany

[‡]Institute of Laser Technologies in Medicine and Metrology, Ulm University, Helmholtzstrasse 12, 89081 Ulm, Germany

[§]University Medicine of the Johannes Gutenberg University, III. Medical Clinic (Hematology, Oncology and Pulmonology), Langenbeckstrasse 1, 55131 Mainz, Germany

Supporting Information

ABSTRACT:

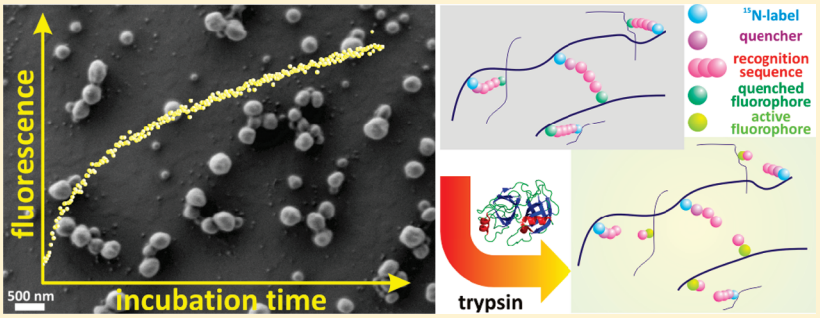

Here we present the synthesis of site specific, protease (trypsin) cleavable, hydrophobic peptide−polymer conjugate nanoparticles in inverse miniemulsion. Different peptide sequences were synthesized by microwave-assisted solid-phase synthesis and characterized by HPLC, NMR, and MALDI-TOF MS. The peptides were used to cross-link a hydrophobic functional polymer with standard peptide-coupling chemistry in inverse miniemulsion, thus generating the desired nanoparticulate morphology. By these means, well-defined nanoparticles in the size range of 200−300 nm were obtained. After transferring the particles into aqueous medium, they were characterized with photon cross-correlation spectroscopy (PCCS) and scanning electron microscopy (SEM). After removal of the solvent, the degree of cross-linking was determined by ^{15}N solid-state NMR. Integration of a fluorophore/quencher system, based on fluorescence resonance energy transfer (FRET) in the peptide sequences, enabled the monitoring of site specific recognition of cross-linked polymeric nanostructures by enzymes, resulting in a fluorescence recovery upon cleavage of the peptide.

INTRODUCTION

Increasingly interesting classes of hybrid materials are peptide−polymer conjugates, where a peptide is covalently attached to a polymer. The hybrid material benefits from the synergism of both components, leading to significantly improved or totally new properties, like optimized solubility,[1] increased blood circulation time,[2] or self-assembling structures.[3] Therefore, numerous applications for this class of materials, such as drug delivery systems,[4] bioactive hydrogels,[5] or additives for directing mineralization,[6] emerge in fields like material science, medicine, or biotechnology. This topic is addressed extensively in several reviews.[7−10]

The first report of a peptide−polymer conjugate consisting of polyvinylpyrrolidone (PVP) and glycylleucine dates back to 1954.[11] Subsequently peptide−polymer conjugates with bovine serum albumin (BSA) and poly(ethylene glycol) (PEG) have been described.[12] As PEGs are easily accessible and water-soluble, they meanwhile act as the most prominent and best established polymeric part of these hybrid materials.[13−15]

In principle, there are three different strategies for conjugate synthesis. The direct coupling of a peptide to a matching functional group of a polymer (polymer analogous reaction) is widely applied. This can be achieved, for example, via thiol addition,[16] Staudinger ligation,[17] cycloaddition,[18] peptide coupling chemistry,[19] or many other reactions.[20] Furthermore, conjugates can be prepared by controlled polymerization from peptide macroinitiators or peptide synthesis on a synthetic polymer. This can be accomplished either by atom transfer radical polymerization (ATRP),[21] nitroxide-mediated radical polymerization (NMRP),[22] and reversible addition−fragmentation chain transfer (RAFT)[23] or by

Received: May 19, 2011
Revised: July 19, 2011
Published: July 29, 2011

grafting the peptide from a solid supported[24] or soluble polymer.[25] The third possibility is the copolymerization of a monomer with a peptide macromonomer (grafting through).[26]

Regarding this synthetic toolbox, the most straightforward approach is the employment of the well-established peptide coupling chemistry (active ester synthesis)[27] for the synthesis of peptide−polymer conjugates. As the necessary reagents have constantly been improved over decades to be highly efficient, this approach seems to be very promising.

By choosing a peptide for conjugate synthesis, which is selectively recognized by a specific enzyme, site specific, degradable hybrid materials can be designed. Promising, cheap, and versatile candidates for a model system for enzyme-responsive peptide−polymer conjugates are proteases like pepsin (pH 1.5−4) and trypsin (pH 7−9). Easy application, availability in great quantities, and existence of degradable peptide sequences make them perfect model candidates.

Trypsin (EC 3.4.21.4) is a serine protease appearing in the mammalian small intestine. Pepsin A (EC 3.4.23.1) is an aspartic protease appearing in the stomach of humans and other mammals. They preferentially cleave proteins or peptides between two aromatic amino acids like tryptophan, tyrosine, and phenylalanine. The shortest peptide sequence reported to be cleaved by pepsin is Gly-Phe-Phe-OEt (GFF-OEt).[28]

One interesting class of such degradable conjugates are enzyme-responsive materials.[29] So far, the majority of enzyme-responsive peptide polymer conjugates are based on hydrophilic polymers, like PEG.[5,30−32] A major drawback of the hydrophilic systems is the difficulty to achieve controlled release from PEG hydrogels as leakage or diffusion may take place in physiological (aqueous) medium from such structures. Therefore, hydrophobic polymers might be used to overcome these disadvantages, as it is even possible to fully encapsulate and protect hydrophobic functional substances. Up to date only few references dealing with peptide−polymer conjugates based on hydrophobic polymers can be found.[33,34] Polystyrene might be a suitable model for hydrophobic polymers, as synthetic methods and analytics are well developed.

In addition to the synthesis of peptide−polymer conjugates, their formulation to nanostructures in water is beneficial as for possible applications, aqueous dispersions are convenient to handle. A very versatile method for the formation of nanoparticulate polymer structures and efficient encapsulation of a broad range of substances is the miniemulsion process.[35] It can be applied to synthesize hydrophobic as well as hydrophilic nanoparticles, featuring a wide variety of polymers. As within this paper exclusively the inverse process is employed, this concept is briefly explained. A typical inverse miniemulsion is composed of a hydrophobic continuous phase (e.g., cyclohexane), a hydrophilic dispersed phase (e.g., water or *N*,*N*-dimethylformamide), and an emulsifier with a low hydrophilic−lipophilic balance (HLB < 7; e.g. an amphiphilic block copolymer), stabilizing the small droplets generated by high shear as e.g. ultrasonication. By adding a hydrophilic costabilizer to the dispersed phase, diffusional degradation through Ostwald ripening is suppressed. Thus, even during reactions, the relative compositions of the droplets remain constant,[36−38] as long as no components with a high solubility in the continuous phase are present.

Compared to other approaches to generate nanoscale-sized enzymatically cleavable particles, like nanolithography on small quartz templates,[39] nanoparticle formation in inverse miniemulsion is quick and conveniently performed with common lab equipment[40] up to a multiliter scale.

Scheme 1. Concept of Enzyme-Degradable Nanoparticles

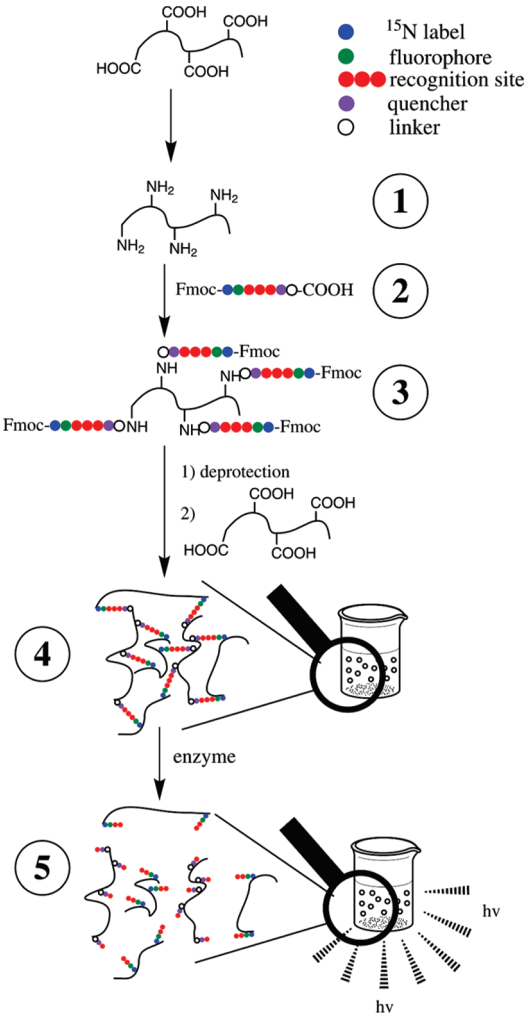

Here we present the preparation of site-selective, protease-cleavable, hydrophobic peptide−polymer nanoparticles. The cleavable peptide sequence was designed to contain three distinctive features. The first one is the recognition site for the protease, the second is a system for *in situ* monitoring of enzymatic cleavage, consisting of a fluorophore and a quencher (FRET pair) enclosing the recognition site, and the third is a probe for successful coupling to the polymer (cross-linking) which is realized by a ^{15}N-label at the peptide's N-terminus. A general overview over the synthetic route is shown in Scheme 1. The peptide sequence and the corresponding complementary polymers were covalently coupled by standard peptide coupling chemistry. Afterwards, these conjugates were cross-linked in inverse miniemulsion to obtain nanoparticles. After transferring the particles into aqueous medium, the cross-linking peptides were successfully cleaved by trypsin. By measuring fluorescence recovery of the FRET system incorporated into the peptide part of the conjugate, cleavage was monitored *in situ*.

RESULTS AND DISCUSSION

Concept. Five relevant aspects for the design and synthesis of the hydrophobic, enzymatically degradable polystyrene−peptide nanoparticles had to be considered (see Scheme 1): (1) synthesis

of complementary polymers with functionalities suitable for peptide coupling chemistry, (2) identification and synthesis of a suitable recognition sequence for the protease with an incorporated detection label, (3) coupling of the two materials to the peptide−polymer conjugates, (4) formation of nanostructures, and (5) enzymatic heterophase degradation and monitoring by fluorescent recovery.

The general concept will be introduced briefly: In order to be able to employ classic peptide chemistry, the polystyrene (PS)-based polymers were designed to match the reactive groups of either the C- or N-terminus of any peptide backbone. Carboxy-functionalized PS with a molecular weight of 5000 g mol^{-1} was synthesized by employing acrylic acid as comonomer via free radical polymerization. To obtain the polymeric amino counterpart, this polymer was converted into an amino-functionalized PS (see Scheme 1, **1**). Thus, the degree of polymerization as well as the number and distribution of functionalites was retained.

As recognition site, a short and thus easily accessible peptide sequence (Gly-Phe-Phe/GFF, Scheme 1, highlighted in red) was chosen. The corresponding, readily available and cheap enzymes pepsin and trypsin are regarded as a well-suited model system for a proof of concept study. As the sequence only has two functional groups (terminal −COOH and $-NH_2$), which can be protected orthogonally, it is an excellent choice for the convenient formation of well-defined peptide−polymer conjugates. To guarantee coupling selectivity by employing well-established peptide coupling chemistry during synthesis of peptide−polymer conjugates, the peptide was designed in such manner, that only one peptide functionality is present in each synthetic step. Therefore, one terminus of the peptide needs to be protected (see Scheme 1, **2**). Protecting groups of either C-terminus (R-COOEt) or N-terminus (Fmoc-NHR) have to be applied accordingly.

For the detection of the enzymatic degradation, a fluorophore/quencher pair, a so-called FRET (fluorescence resonance energy transfer)[41] system (see Scheme 1, highlighted in green and purple), was introduced into the peptide sequence. Emission upon excitation of the donor (fluorophore) remains unimpaired as long as the distance to the acceptor (quencher) is significantly greater than the Förster radius (1−8 nm).[42] Decrease of the distance between donor and acceptor will result in nonradiative energy transfer from the donor to the acceptor (quenching). In the intact peptide sequence, the mutual distance is well below the Förster radius, and thus FRET, which is a common tool in the detection of enzymatic activity,[43] is highly effective. Cleavage of the peptide sequence will lead to a fluorescence signal due to the increasing distance between donor and acceptor that can be detected *in situ*. Monitoring of the coupling efficiency between peptide and polymer during synthesis of nanostructures was achieved by the introduction of a ^{15}N-label on the N-terminus of the peptide, (see Scheme 1, highlighted in blue). By this means, it was possible to monitor the change from (uncoupled) amino groups to (coupled) amide groups by ^{15}N solid-state NMR.

Because of the availability of carboxyl or amino groups, the polymers can be conjugated to either the C- or N-terminus of a peptide. Consequently C-terminal coupled conjugates ("Fmoc−NH−peptide−polymer") were synthesized (see Scheme 1, **3**).

The N-terminal coupled conjugates ("polymer−peptide−COOEt") are not shown in Scheme 1 as they were just synthesized to clarify if coupling of a peptide to the polymer is possible and to identify the nature of bulk cleavage products. Synthesis of N-protected peptides was pursued for nanoparticle preparation (see Scheme 1, **4**), as they can be modified conveniently by applying solid phase peptide synthesis (SPPS). After attachment of the peptide to the polymer and removal of the Fmoc-protecting group, a peptide−polymer conjugate is obtained. Subsequent coupling of the corresponding polymer leads to peptide-cross-linked PS. By employing ^{15}N-labeled peptides, it is possible to monitor the cross-linking reaction between polymer and peptide−polymer conjugate and to determine the degree of cross-linking in that step.

Synthesis. *1. Polymer Synthesis.* The polymer will play a crucial role in the cleavage of the desired nanoparticles. The cross-linked particles should not be soluble or swell too much in water on the one hand, but on the other hand, the fragments of the particles should dissolve after enzymatic degradation. Consequently statistic copolymers of styrene and acrylic acid (PS-*co*-PAA) were synthesized by free radical polymerization in ethanol. With the copolymerization parameters of both components in ethanol (styrene: $r_s = 0.31$; acrylic acid: $r_{AA} = 0.19$)[44] the formation of a statistic copolymer can be expected. This was confirmed by SEC and NMR (see Supporting Information). The polymer's structure was verified by ^1H NMR and ^{13}C NMR. The molecular weight (M_w) was 5000 g mol^{-1}. The PDI was usually 1.9.

NMR and volumetric analysis were chosen in order to determine the composition of the copolymer. Aromatic peaks and the acid peak were chosen for integration (see Supporting Information S1). In addition to the determination of the copolymer composition by NMR, the content of functional groups in the polymer was quantified by titration with 0.1 M NaOH in THF/H_2O.

The amount of acrylic acid units in the polymer obtained by ^1H NMR was 7.1 ± 0.6 wt %, whereas the result obtained by titration was 8.4 ± 1 wt %. Thus, both methods led to similar results within the margin of error.

In order to guarantee well-defined and controlled synthesis of nanoparticles, the carboxy- and the amino-functionalized polymers should be as similar as possible. The best way to obtain a similar amino-functionalized counterpart with respect to molecular weight, molecular weight distribution, and amount of functional groups is to perform a polymer-analogous reaction with carboxy-functionalized polystyrene. Thus, PS-*co*-PAA was converted into an amino-functionalized polymer by employing peptide coupling chemistry with mono Boc-protected ethylenediamine (Boc-NH-C_2H_4-NH_2). A negative ninhydrin test after the coupling reaction excluded possible free amine in the product and indicated quantitative reaction. After removal of the Boc-protection group, amino-functionalized polystyrene—(PS-*co*-PAA)-C_2H_4-NH_2—was obtained. The structure was verified by ^1H NMR and ^{13}C NMR. After the polymer analogous reaction M_w increased to 9500 g mol^{-1}. The PDI was 1.8. As no identical SEC standards were available and the copolymers contained about 90% polystyrene, pure polystyrene was chosen as reference. Therefore, the molecular weight should not be taken as "real" value, but as indication for successful reaction. As deprotection was performed by treatment with HCl, the amino-functionalized polymer was obtained as hydrochloride. In this case titration for quantification of degree of functionalization is not accurate, as residual HCl leads to overestimated values. Therefore, the composition of the copolymer was determined by ^1H NMR. The theoretical value calculated from the starting material, assuming quantitative reaction, was 10.9 ± 1.0 wt %. The experimental data obtained by ^1H NMR was 10.3 ± 0.6 wt %. Both values are similar within the margin of error. This indicates that the coupling efficiency was quite high. A reason for

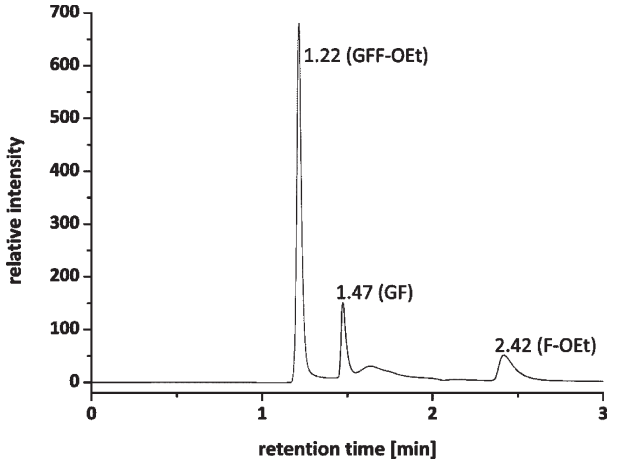

Figure 1. Enzymatic cleavage products (GF, F-OEt) of GFF-OEt after 74 h treatment with pepsin.

the discrepancy can be the possible limited accessibility of some functional groups due to steric hindrance in the polymer.

By this procedure, polymers bearing similar numbers of functional groups, similar molecular weight and similar molecular weight distribution were synthesized. Considering further synthesis, SEC data are dispensable, as it is impossible to provide adequate standards for the peptide−polymer conjugates.

2. Identification of the Appropriate Peptide Sequence: Synthesis and Adaption. First, the shortest reported pepsin/trypsin-cleavable peptide (H_2N-GFF-OEt)[28] was synthesized in solution, as C-terminal protected peptides are not accessible with SPPS. A standard Boc-protocol[45] was employed, using *N,N′*-dicyclohexylcarbodiimide (DCC), 1-hydroxy-1*H*-benzotriazole (HOBt), and triethylamine as activating agents and the respective Boc- and ethyl-protected amino acids. After each coupling step the Boc-deprotection was achieved by treatment with 1.4 M HCl in ethyl acetate.

All intermediates were purified and then characterized by NMR, HPLC, and MALDI-TOF MS. Following this route, H_2N-GFF-OEt was synthesized successfully. The peptide was degraded by treatment with pepsin, and the nature of the cleavage products was investigated by HPLC (see Figure 1).

The data clearly show that the degradation of H_2N-GFF-OEt (t_{ret} = 1.22 min) took place and two additional peaks appeared at t_{ret} = 1.47 min and t_{ret} = 2.42 min after 74 h of incubation. By comparing the elution times with the respective standards, glycyl-L-phenylalanine (t_{ret} = 1.47 min) and L-phenylalanine ethyl ester hydrochloride (t_{ret} = 2.42 min) were identified as the cleavage products. The enzyme cleaved the sequence between the aromatic amino acids phenylalanine, as expected from the literature,[28] making it suitable as enzyme recognition sequence for further investigation. Thereafter, SPPS was employed for further synthesis as a modification of the motif can be achieved more easily.

During the synthesis of the following peptides standard Fmoc-protocol for SPPS was employed. The peptide's structures were confirmed by MALDI-TOF MS and NMR. Purity was verified by HPLC and estimated as more than 95%. An overview of the peptides employed here can be found in Chart 1.

Detection and analysis of the cleavage products with HPLC is accurate and is the method of choice to identify the cleavage products of short sequences. However, it becomes increasingly difficult for multiple cleavage products, as expected from highly cross-linked peptide−polymer conjugates. Furthermore, HPLC is not suitable for *in situ* detection of the enzymatic cleavage. Incorporation of a fluorophore/quencher pair in the peptide, enclosing the recognition site is particularly useful as fluorescence increases through degradation of the peptide.

Ideally, the recognition motif should only be changed minimally by the introduction of the FRET label, in order to ensure selective and sensitive recognition. Therefore, a small fluorophore, anthranilic acid (Ant), was chosen in combination with the suitable quencher 3-nitrotyrosine (Y_N).[46] To prove the ability to cleave the peptide, Ant-GFF-Y_NG-OH was synthesized on solid phase (see Chart 1). After treatment with trypsin the fluorescence increased, showing successful cleavage of the peptide (see Figure 2).

For the defined use in SPPS, anthranilic acid had to be protected with Boc. This implies that it can only be introduced in the last step, as no functional group is left for further reaction. This restricts the labeling to the peptide's N-terminus. Consequently, possibilities to incorporate the fluorophore in variable positions were investigated. More flexibility in terms of synthesis can be gained by decoupling the fluorophore from the peptide's backbone and to attach it via an α-amino acid linker, like lysine (K). Thus, the fluorophore can be incorporated in any desired position of the peptide, without severe disturbance of the recognition site. Thus, Y_N-GFF-K_{Ant}-G-OH was synthesized and evaluated in a cleavage experiment. Although the quenching was efficient and the fluorescent recovery satisfactory, the amino group of anthranilic acid is prone to side reactions, and thus a protection of the functional group is necessary. One possibility was methylation of the amine group in anthranilic acid, yielding *N*-methylanthranilic acid (Mant).

With Fmoc-L-Lys(Mant)-OH (K_{Mant}) being synthesized successfully, Y_N-GFF-K_{Mant}G-OH (see Chart 1) was only obtained within a mixture of products. The same effect was observed during the synthesis of (^{15}N)GK_{Mant}-GFF-Y_NG-OH. Without further purification by preparative HPLC, (^{15}N)GK_{Mant}-GFF-Y_N-G-OH was only obtained as a mixture of two peptides. Surprisingly, the methyl group does not efficiently protect the amino group of the fluorophore from further coupling steps. This leads to an increasing number of side products with every elongation step of the peptide. Full protection of the amine by complete methylation was not possible, as the product does not show fluorescence.[47] As derivatives of anthranilic acid were not suitable as universally applicable fluorophore (see Supporting Information), the system had to be changed to the larger fluorophore 7-methoxycoumarin-4-acetyl (Mca) and its corresponding quencher 2,4-dinitrophenyl (Dnp).[43] Both components are used attached to a linker—Fmoc-L-lysine—to guarantee high flexibility and therefore efficient quenching, leading to an excellent ratio of fluorescence between the cleaved and the noncleaved state.[48] Furthermore, total freedom in terms of peptide design is now achieved, as both components can be integrated into any position of the peptide sequence.

The synthesis was conducted employing Fmoc-L-Lys(Mca)-OH and Fmoc-L-Lys(Dnp)-OH, and the peptide (^{15}N)-G-K_{Mca}-GFF-K_{Dnp}G-OH (see Chart 1) was obtained in high yields and was successfully degraded by trypsin (see Figure 2).

By comparing the gray curve corresponding to Ant-GFF-Y_NG-OH (relative fluorescence maximum 4.3) and the black one corresponding to (^{15}N)-G-K_{Mca}-GFF-K_{Dnp}G-OH (relative fluorescence maximum >5.5) in Figure 2, it is clearly visible that the

Chart 1. Overview of Employed Peptide Sequences

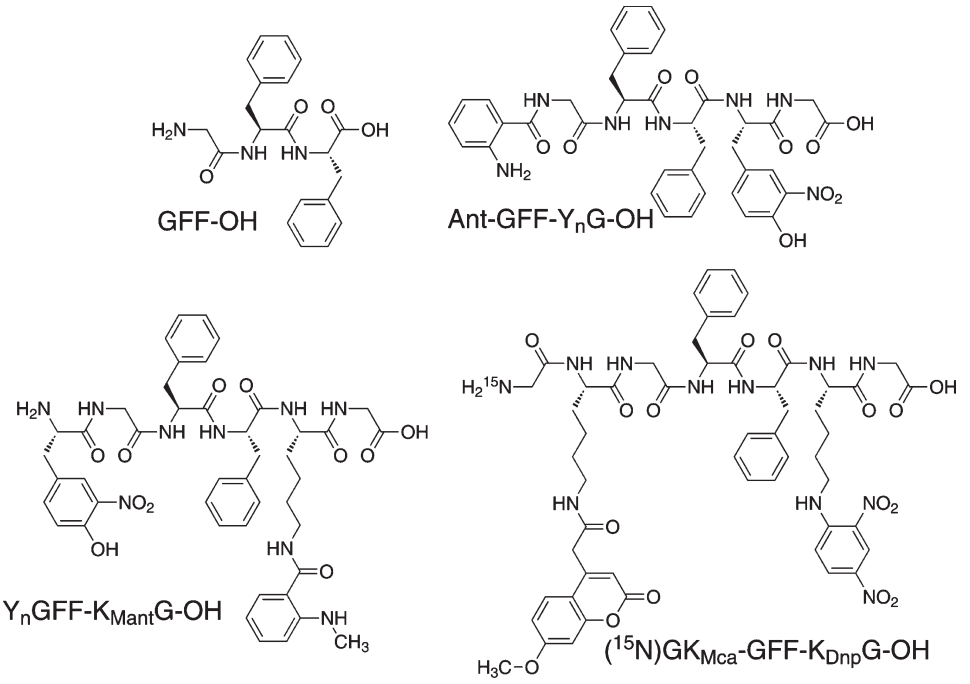

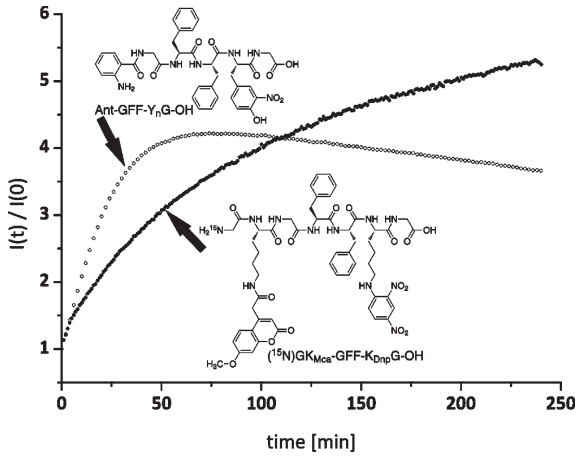

Figure 2. Relative fluorescence increase upon enzymatic cleavage of Ant-GFFY$_N$G-OH and (^{15}N)-G-K$_{Mca}$-GFF-K$_{Dnp}$G-OH by trypsin. The relative fluorescence is normalized to the fluorescence occurring at $t = 0$.

fluorescence increase was higher by introduction of the Mca/Dnp system. However, degradation of Ant-GFF-Y$_N$G-OH is faster than the degradation of (^{15}N)-G-K$_{Mca}$-GFF-K$_{Dnp}$G-OH. This might be due to better accessibility of the peptide's recognition site upon usage of the small fluorophore.

The decrease of the gray signal (Ant) after 60 min can be attributed to photo bleaching of the fluorophore, which further favors the use of Mca (black signal).

Monitoring of the coupling to the polymer was achieved by ^{15}N- labeled glycine, incorporated at the N-terminus of the peptide. Thus, the reaction of the amino group to an amide bond can be monitored by ^{15}N NMR.

With the peptide Fmoc-(^{15}N)G-K$_{Mca}$-GFF-K$_{Dnp}$-G-OH, all required features are eventually realized in one sequence (see

Scheme 2. ^{15}N-Labeled, Fluorescent Quenched, Cleavable Peptide Sequence

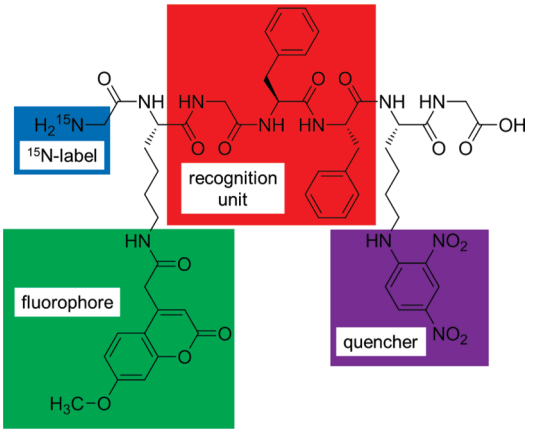

Scheme 2): the ^{15}N-label for detection of successful cross-linking, the recognition site for enzymatic degradation (GFF), and the fluorophore/quencher pair (Mca, Dnp) for its detection.

3. Synthesis of Peptide—Polymer Conjugates. Following a route not shown in Scheme 1, H$_2$N-GFF-OEt was coupled to carboxy-functionalized polystyrene using DCC/HOBt/triethylamine as activating agents. After liberation of the acid upon deprotection with sodium hydroxide (PS-*co*-PAA)-GFF-OH was synthesized successfully. By pursuing that synthetic route, it was possible to couple the N-terminus of the peptide to the carboxyl-functionalized polymer.

Alternatively, Fmoc-GFF-OH was conjugated to amino-functionalized PS (see Scheme 1, **3**). Thus, it was also shown that the attachment of the C-terminus of a peptide to the respective

dx.doi.org/10.1021/ma201149b |*Macromolecules* 2011, 44, 6258–6267

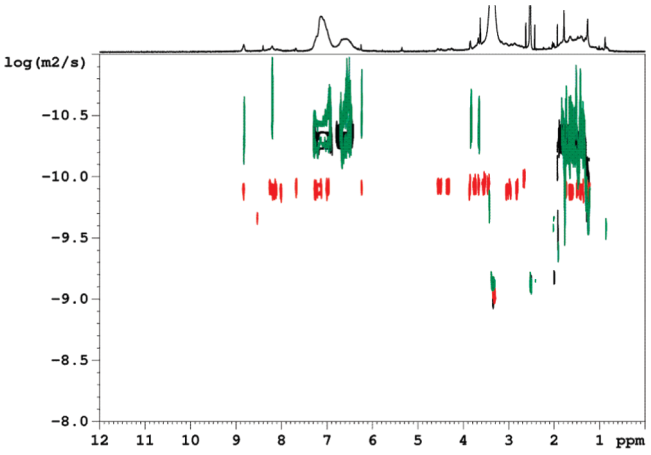

Figure 3. Overlay of three DOSY-NMR spectra: (PS-*co*-PAA)-C_2H_4-NH-GK_{Dnp}-FFG-K_{Mca}G-$^{15}NH_2$ in green, PS-*co*-PAA in black and HO-GK_{Dnp}-FFG-K_{Mca}G-$^{15}NH_2$ in red (700 MHz, DMSO-d_6, 289.3 K).

polymer is possible. The structures of the peptide−polymer conjugates were confirmed by ^{1}H NMR and ^{13}C NMR.

These results demonstrate that a successful coupling can be achieved via the peptide's N- and C-terminus. As mentioned above, SPPS conveniently works for Fmoc-protected NH_2 termini; thus, the route shown in Scheme 1 was further pursued.

To guarantee *in situ* detection of enzymatic cleavage, the FRET pair labeled sequence Fmoc-(^{15}N)G-K_{Mca}-GFF-K_{Dnp}-G-OH was coupled to amino-functionalized polystyrene using (1-cyano-2-ethoxy-2-oxoethylidenaminooxy)dimethylaminomorpholinocarbenium hexafluorophosphate (COMU)[27] and 2,4,6-trimethylpyridine (TMP) as activating agents. After removal of the Fmoc-group, (PS-*co*-PAA)-C_2H_4-NH-GK_{Dnp}-FFG-K_{Mca}G-$^{15}NH_2$ was obtained. The structure of the conjugate was confirmed by ^{1}H NMR and ^{13}C NMR.

In addition, the success of the reaction can be clearly seen by employing "diffusion ordered spectroscopy" (DOSY) NMR. With that method it is possible to measure the diffusion coefficient (D, [$m^2\ s^{-1}$]) of molecules and correlate them to the distinctive ^{1}H-pattern of protons of the investigated molecule. Here an overlay of three spectra is correlated to the product's ^{1}H spectrum (see Figure 3).

The signals of the pure peptide corresponding to a diffusion coefficient of 1.268×10^{-10} $m^2\ s^{-1}$ are highlighted in red. The signals of the pure polymer ($D = 4.966 \times 10^{-11}$ $m^2\ s^{-1}$, black) and the signals of the peptide−polymer conjugate ($D = 4.436 \times 10^{-11}$ $m^2\ s^{-1}$, green) have lower diffusion coefficients than the pure peptide, corresponding to a molecule with higher hydrodynamic diameter (d_H). This observation can be attributed to the successful attachment of the peptide to the polymer and the resulting increase of the hydrodynamic radius of the conjugate compared to the polymer. This is underlined by the fact that the signals of the peptide (e.g., 4.3 and 4.5 ppm) and the signals of the polymer (e.g., 1.6 and 6.7 ppm) appear in the green spectrum at the same diffusion coefficient. The different amounts and signal intensities of some protons cause their absence in the conjugate's signals shown in Figure 3.

This clearly illustrates successful coupling, which is supported by results of HPLC analysis (see Figure 4), where only one broad signal (t_{ret} = 7.9 min) attributed to the conjugate and no free peptide (t_{ret} = 6.2 min) was observed in the chromatogram.

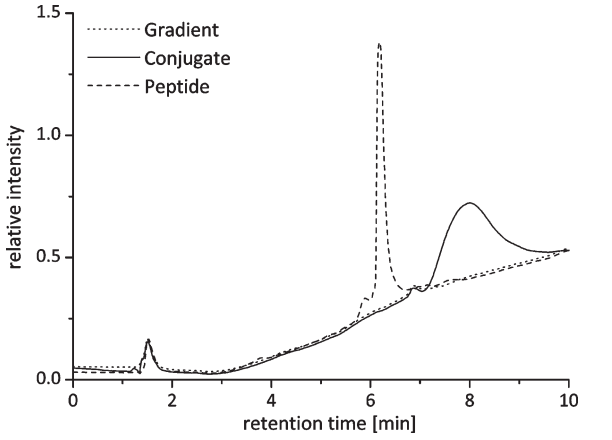

Figure 4. HPLC of (PS-*co*-PAA)-C_2H_4-NH-GK_{Dnp}-FFG-K_{Mca}G-$^{15}NH_2$ and reference peptide.

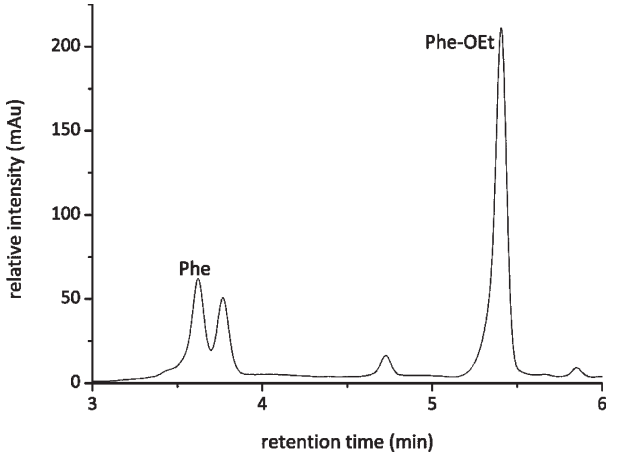

Figure 5. Cleavage products (Phe-OEt, Phe) of micrometer-sized particle's treatment of (PS-*co*-PAA)-GFF-OEt with pepsin.

Peptide content in the conjugate was determined with quantitative ^{1}H NMR, employing the sodium salt of 3-trimethylsilyl-1-propanesulfonic acid (DSS (4,4-dimethyl-4-silapentane-1-sulfonic acid) as reference substance. In the resulting spectrum the integral of the methyl peak (R-Si-$(CH_3)_3$, 0.03 ppm) of the reference was set to 9. The resulting integral of a well-separated peak (Gly: −NH−C*H*H−CO−, 4.55 ppm) of the peptide was used to calculated the ratio of peptide in the sample. According to the initial mass of DSS and the mass of the conjugate, the ratio between polymer and peptide was calculated. The peptide content was determined to be 42 wt % (theoretical 61 wt %). The theoretical value differs from the experimental, indicating incomplete conversion. The most probable reason for the incomplete reaction is steric hindrance of the fluorophore resulting in lower peptide coupling.

4. Nanostructure Formation and Enzymatic Degradation. Proteases normally work on proteins in the nanometer range, in solution (homophase). However, it is also known that enzymes are able to catalyze reactions on surfaces (heterophase).[49−51] Nevertheless, it had to be ensured that the heterophase micro- or nanostructures synthesized here can also serve as substrates. This includes the question of whether the conjugate's peptides are accessible for the enzyme at all. Micron-sized particles were

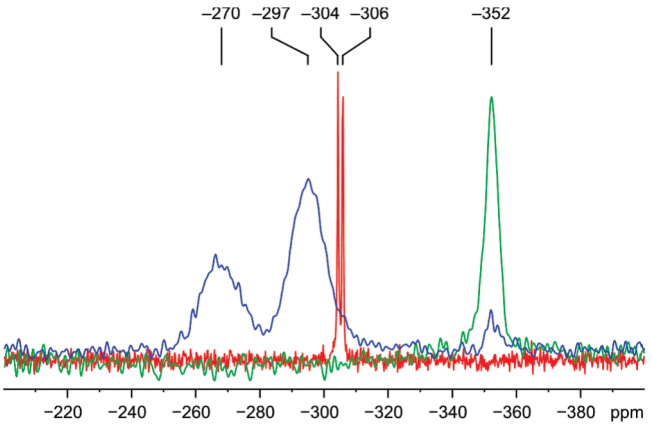

Figure 6. Solid-state ^{15}N-spectra of unreacted amine "(PS-*co*-PAA)-C_2H_4-NH-GK$_{Dnp}$-FFG-K$_{Mca}$G-$^{15}NH_2$" (green), product amide "polymer-peptide-^{15}NCO-polymer" (blue) and reference amide "Fmoc-(^{15}N)-Gly" (red), 30.4 MHz, 289.3 K.

Table 1. Particle Size before and after Dialysis (PCCS)

before dialysis	X_{10}	X_{50}	X_{90}
[nm]	190	220	260
after dialysis	X_{10}	X_{50}	X_{90}
[nm]	200	230	270

prepared by ultrasonic disintegration of the bulk conjugate—(PS-*co*-PAA)-GFF-OEt—in water. The accessibility of the sequences present on the structure was shown by successful cleavage (see Figure 5) by pepsin. The peaks were compared with standards (Phe-OEt, Phe) to evaluate their identity. This finding shows that proteases are indeed active on the present heterophase substrates.

Thus, it was demonstrated that the conjugates coupled from one side to the water-insoluble polymer can be degraded by a protease. As already mentioned above, for larger structures, especially for cross-linked nanoparticles, HPLC is not suitable for the detection of cleavage products, as the formation of small soluble products cannot be expected. Thus, the FRET system was used for further studies.

The formulation of hydrophobic peptide cross-linked polystyrene nanoparticles was achieved in inverse miniemulsion. This process is a powerful tool for the formation of defined nanostructures.[52] So far it was mainly used for the preparation of capsules or inorganic nanoparticles[38,40,53] and high-temperature polymerization.[54] Here, we employed DMF as hydrophilic organic, disperse phase, as it is a suitable solvent for the peptide, the polymer, the peptide−polymer conjugates and the necessary reagents. As continuous phase isooctane was chosen, as it is not miscible with DMF. Successful reaction was controlled with the incorporated ^{15}N-label. To evaluate the reaction properties and parameters for the miniemulsion process, the reaction was first performed in bulk. The parameters established in the bulk synthesis were used for the inverse miniemulsion process. (PS-*co*-PAA)-C_2H_4-NH-GK$_{Dnp}$-FFG-K$_{Mca}$G-$^{15}NH_2$, PS-*co*-PAA, and COMU were dissolved in DMF/*N*-methyl-2-pyrrolidone and nanometer-sized droplets in isooctane were generated by ultrasound. The coupling reaction was initiated by the addition of *N,N*-diisopropylethylamine through the continuous phase. As branched polymers are employed, swollen cross-linked particles

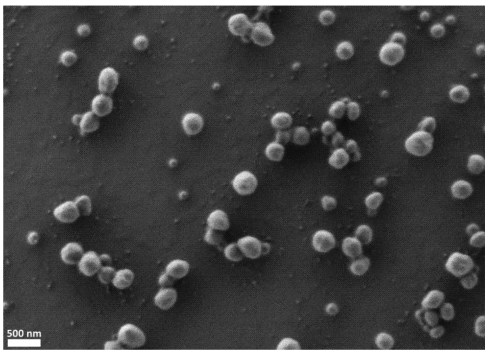

Figure 7. SEM image of cross-linked particles.

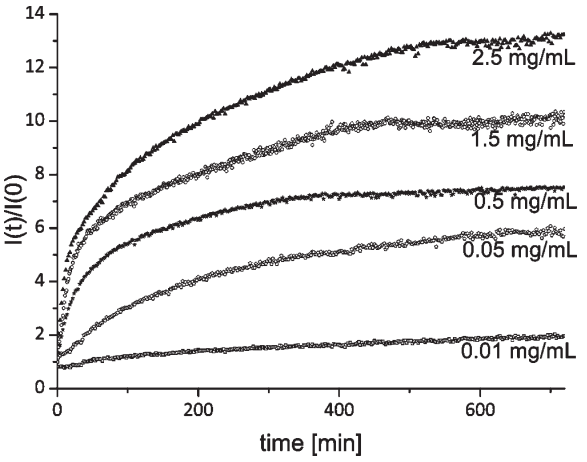

Figure 8. Particle degradation, employing varying concentrations of trypsin.

were obtained. Afterwards, the inverse miniemulsion was transferred in an aqueous sodium dodecyl sulfate (SDS) solution. After purification, parts of the sample were freeze-dried for the ^{15}N-solid state NMR measurement.

With the ^{15}N-label, the transformation of unreacted amine to an amide product was monitored conveniently. As cross-linked, insoluble structures were obtained, ^{15}N solid-state NMRs of the samples before and after reaction were measured. Fmoc-L-(^{15}N)-glycine (δ = −304, −306 ppm) served as reference amide.

In Figure 6, an overlay of the ^{15}N-spectra of unreacted amine "(PS-*co*-PAA)-C_2H_4-NH-GK$_{Dnp}$-FFG-K$_{Mca}$G-$^{15}NH_2$" (green), product amide "polymer-peptide-^{15}NCO-polymer" (blue), and reference amide "Fmoc-(^{15}N)-Gly" (red) is presented. In the green spectrum a single peak at −352 ppm is observed, which disappears after reaction (blue spectra), while two new peaks appear at −270 and −297 ppm in the blue spectrum. In comparison with a model amide, Fmoc-^{15}N-glycine (−304 and −306 ppm, red spectrum), this low-field shift clearly confirms the amide formation and therefore the successful cross-linking of the polymer. From the spectrum of the product, the conversion (cross-linking) can be estimated to be about 90%. HPLC samples did not dissolve at all, and no signal was obtained, supporting the results of solid-state NMR that no "free" peptide is present in the dispersion.

The cross-linked particles in aqueous phase (before freeze-drying) were characterized for their colloidal properties. The

dx.doi.org/10.1021/ma201149b |*Macromolecules* 2011, 44, 6258–6267

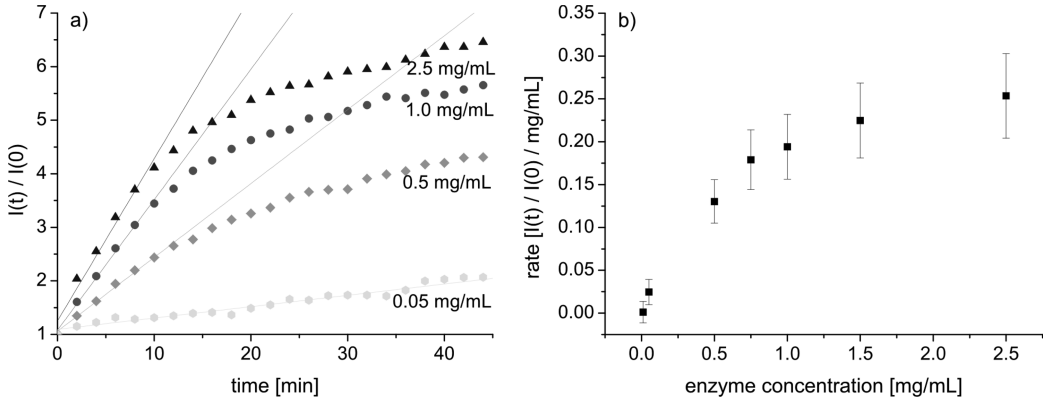

Figure 9. (a) Linear fits for initial enzymatic degradation rate of particles (enlargement of Figure 8). (b) Dependency of particles' degradation rate on trypsin concentration.

particle size in aqueous medium was determined by photon cross-correlation spectroscopy (PCCS). The results of the measurement before and after dialysis are shown in Table 1. The particle size did not change during dialysis. The X_{50} value (50% of the particles below that value) was 230 nm. This value was confirmed by SEM (see Figure 7).

Electron micrographs revealed spherical particles with the same size distribution as determined by PCCS. From the micrographs an average size of 238 nm was determined. The zeta-potential was −2.96 mV and the solids content of the dispersion 1 wt %.

After the continuous phase was changed to aqueous conditions, degradation experiments were performed. In order to conduct the enzyme-induced degradation of the nanoparticles, the dispersions were diluted using phosphate buffered saline (PBS^-). Solutions of trypsin with varying concentration were added to the stable dispersion, resulting in concentrations ranging from 0.01 to 2.5 mg mL^{-1}. The time course of the fluorescence intensity was monitored in order to investigate the cleavage process (see Figure 8).

These results clearly demonstrate that the nanoparticles were degraded by trypsin. Fluorescence intensity increased with rising incubation time and rising enzyme concentration. Treatment of the particles with other enzymes like dextranase or lipase did not result in a fluorescence increase, showing that the particles are specifically degraded by proteases.

In order to calculate the conversion rate for each enzyme concentration, a series of linear fits of the initial rate data points of Figure 8 were performed (see Figure 9a). The resulting slopes, representing the cleavage rates of the reaction, were furthermore plotted against the enzyme concentration (see Figure 9b).

Figure 9b shows a linear increase of the cleavage rate (<0.5 mg mL^{-1}) until it flattens to an asymptotical value. This result is contrary to an effect appearing in enzymatic esterification in heterophase.[55] Therefore, the results indicate that inhibitory effects start to occur at enzyme concentrations of about 0.5 mg mL^{-1}, as the curve deviates from the linear course. The observation can be explained by the fact that in the system only a limited amount of surface area, where the reaction occurs, is available. Although a great amount of peptide is located in the particles, only the cleavable sites on the surface can be accessed by the enzymes. Moreover, nonreversible surface coverage by adsorbed enzymes might occur. An estimation was used to approximate which concentration of protease would lead to complete surface coverage of the nanoparticles. For this assumption the surface occupied by each molecule was calculated as a disk with a radius equal to the radius of the enzyme. Using the hydrodynamic radius of trypsin (2 nm)[56] as well as the surface area of the particles shows that the deviation from the linear behavior becomes evident between 0.05 and 0.5 mg mL^{-1}, which corresponds quite well with the data observed in Figure 9b. SEM and PCCS data after enzymatic degradation underlined the inhibitor effect. The data also showed that the particles did not degrade completely.

For common enzymatic degradation experiments in solution, one would expect comparable values of fluorescence upon total degradation of the substrate for varying enzyme concentrations. The fact that the final intensities for equal amounts of substrates do not result in the same fluorescence intensity further adds to the assumption that there are inhibitory effects. This might also be explained by the general tendency of enzymes to adsorb on particular surfaces possibly rendering them inactive.[57,58] This was confirmed by addition of a defined amount of enzymes in ten steps over time, adding up to the amount previously added in one step. One single addition resulted in an increase of fluorescence to a constant value most probably due to inactivation of the enzyme. Each addition resulted in further increase in fluorescence up to a final intensity comparable to the one step addition of the same enzyme concentration. This supports the aforementioned hypothesis that adsorption and inactivation of the enzyme molecules is the reason for the concentration-dependent final intensity.

CONCLUSION

In this article, the design, synthesis, and degradation of site specific protease cleavable, hydrophobic nanoparticles was presented. We have chosen pepsin and trypsin as model enzymes as they are selective for a certain peptide sequence and readily available. Gly-Phe-Phe (GFF) was employed as the shortest possible recognition sequence. After peptide synthesis in solution for obtaining the N-terminal deprotected sequence and solid phase synthesis of the ^{15}N-, FRET-labeled, C-terminal deprotected sequence, a hydrophobic polymer was synthesized via radical copolymerization of styrene and acrylic acid. The molecular weight of the polymer, with a PDI of 1.9 was 5000 g mol^{-1}. To match the polymer's reactive groups to the C-terminus of the peptide, the carboxylic groups of the polymer were converted into amino groups. Novel peptide−polymer conjugates were

obtained by applying well-established peptide coupling chemistry. After successful deprotection of the polymer coupled peptides, cross-linking of polystyrene via the peptides was achieved and monitored by ^{15}N solid-state NMR. This step was conducted in inverse miniemulsion to obtain nanoparticles with a diameter of 230 nm. After transfer of the particles in aqueous medium, the cross-linking peptides were degraded by trypsin. By making use of a FRET system in the peptide, this was conveniently monitored by increase of fluorescence.

The knowledge derived from this model system provides a basis for future applications in nanomedecine, *in vitro* detection of specific enzymes, or early detection or therapy of cancer.

EXPERIMENTAL SECTION

Detailed information is given in the Supporting Information.

General. DMF (p.a., Sigma-Aldrich), *N*-methyl-2-pyrrolidone (99%, Sigma-Aldrich), and isooctane (99.5%, Applichem) were used as received. COMU (≥98%, Novabiochem) and *N*,*N*-diisopropyethylamine (≥98%, Fluka) were employed as activating agents. For the reaction in inverse miniemulsion the block copolymer emulsifier poly(butylene-*co*-ethylene)-*block*-poly(ethylene oxide) P(B/E-*b*-EO) consisting of a poly(butylene-*co*-ethylene) block (M_w = 3700 g mol^{-1}) and a poly(ethylene oxide) block (M_w = 7300 g mol^{-1}) was synthesized starting from Kraton liquid (Shell), which was dissolved in toluene, by adding ethylene oxide under typical conditions of anionic polymerization.[59] Sodium dodecyl sulfate (SDS, ≥99%, Carl Roth) was employed as emulsifier for the transfer of the inverse miniemulsion into aqueous medium.

Synthesis of Cross-Linked Polymer Particles in Inverse Miniemulsion. For the dispersed phase poly(styrene-*co*-acrylic acid) (13.1 mg, 14.6 μmol COOH) (PS-*co*-PAA)-C_2H_4-NH-GK_{Dnp}-FFG-K_{Mca}-G-$^{15}NH_2$ (38.0 mg, 14.6 μmol NH_2) and COMU (31.8 mg, 73.1 μmol) were dissolved in 456 μL of DMF and 58 μL of *N*-methyl-2-pyrrolidone. 1.54 mL of continuous phase, consisting of 1 wt % solution of P(B/E-*b*-EO) in isooctane, was added. The mixture was preemulsified for 30 min and afterward sonicated for 3 min total sonication time (5 s pulse, 5 s pause) with an 1/8 in. ultrasonication tip (70% amplitude, Branson sonifier 450D) under ice cooling. DIEA (120 μL, 698 μmol) was added, and the reaction mixture was stirred for 15 h at ambient temperature. Afterwards, 8.6 mL of a 0.3 wt % SDS solution was added and treated for 3 min (5 s pulse, 5 s pause) with an 1/2 in. ultrasonication tip (70% amplitude). Isooctane was evaporated by stirring the sample in an open vessel for 48 h at 75 °C. The volume was maintained by adding water. For purification the sample was dialyzed (membrane cutoff: 14 000 g mol^{-1}). The particle size was determined by PCCS before and after dialysis and compared with SEM images. After freeze-drying, successful cross-linking was investigated by ^{15}N solid-state NMR and HPLC.

ASSOCIATED CONTENT

Supporting Information. Materials and Methods, detailed synthesis and characterization of all components. This material is available free of charge via the Internet at http://pubs.acs.org.

AUTHOR INFORMATION

Corresponding Author
*E-mail: landfester@mpip-mainz.mpg.de.

ACKNOWLEDGMENT

This work was supported by the Bundesministerium für Bildung und Forschung (BMBF, grant no. 01 EZ 0806). We thank Petra Kindervater (NMR), Ute Heinz, Sandra Seywald, Christine Rosenauer (SEC), Beate Müller (HPLC), Stephan Türk (MS), and Gunnar Glasser (SEM) for the technical and scientific support.

REFERENCES

(1) Hirsch, A. K. H.; Diederich, F.; Antonietti, M.; Borner, H. G. *Soft Matter* **2010**, *6*, 88.
(2) Abuchowski, A.; McCoy, J. R.; Palczuk, N. C.; Vanes, T.; Davis, F. F. *J. Biol. Chem.* **1977**, *252*, 3582.
(3) Börner, H. G.; Smarsly, B. M.; Hentschel, J.; Rank, A.; Schubert, R.; Geng, Y.; Discher, D. E.; Hellweg, T.; Brandt, A. *Macromolecules* **2008**, *41*, 1430.
(4) Osada, K.; Kataoka, K. *Adv. Polym. Sci.* **2006**, *202*, 113.
(5) Lutolf, M. P.; Raeber, G. P.; Zisch, A. H.; Tirelli, N.; Hubbell, J. A. *Adv. Mater.* **2003**, *15*, 888.
(6) Kasparová, P.; Antonietti, M.; Cölfen, H. *Colloids Surf., A* **2004**, *250*, 153.
(7) Lutz, J.-F.; Börner, H. G. *Prog. Polym. Sci.* **2008**, *33*, 1.
(8) van Hest, J. C. M. *Polym. Rev.* **2007**, *47*, 63.
(9) Krishna, O. D.; Kiick, K. L. *Pept. Sci.* **2010**, *94*, 32.
(10) Gauthier, M. A.; Klok, H. A. *Chem. Commun.* **2008**, *23*, 2591.
(11) Jatzkewitz, H. *Hoppe-Seyler's Z. Physiol. Chem.* **1954**, *297*, 149.
(12) Abuchowski, A.; Vanes, T.; Palczuk, N. C.; Davis, F. F. *J. Biol. Chem.* **1977**, *252*, 3578.
(13) Veronese, F. M.; Harris, J. M. *Adv. Drug Delivery Rev.* **2002**, *54*, 453.
(14) Roberts, M. J.; Bentley, M. D.; Harris, J. M. *Adv. Drug Delivery Rev.* **2002**, *54*, 459.
(15) Duncan, R. *Nat. Rev. Drug Discovery* **2003**, *2*, 347.
(16) Heggli, M.; Tirelli, N.; Zisch, A.; Hubbell, J. A. *Bioconjugate Chem.* **2003**, *14*, 967.
(17) Cazalis, C. S.; Haller, C. A.; Sease-Cargo, L.; Chaikof, E. L. *Bioconjugate Chem.* **2004**, *15*, 1005.
(18) Sander, S. v. B.; Dirks, A. J.; Marjoke, F. D.; Floris, L. v. D.; Jeroen, J. L. M. C.; Roeland, J. M. N.; Floris, P. J. T. R. *ChemBioChem* **2007**, *8*, 1504.
(19) Michal, P.; Brus, J.; Kostka, L.; Konák, C.; Urbanová, M.; Slouf, M. *Macromol. Biosci.* **2007**, *7*, 56.
(20) Heredia, K. L.; Maynard, H. D. *Org. Biomol. Chem.* **2007**, *5*, 45.
(21) Braunecker, W. A.; Matyjaszewski, K. *Prog. Polym. Sci.* **2007**, *32*, 93.
(22) Georges, M. K.; Hamer, G. K.; Listigovers, N. A. *Macromolecules* **1998**, *31*, 9087.
(23) Boyer, C.; Stenzel, M. H.; Davis, T. P. *J. Polym. Sci., Part A: Polym. Chem.* **2011**, *49*, 551.
(24) Rösler, A.; Klok, H.-A.; Hamley, I. W.; Castelletto, V.; Mykhaylyk, O. O. *Biomacromolecules* **2003**, *4*, 859.
(25) Sara, D.; Ilaria, A.; Maurizio, B.; François, M.; Gian, M. B. *Eur. J. Org. Chem.* **2002**, *2002*, 3473.
(26) Hui, D.; Kopeckova, P.; Kopecek, J. *J. Drug Targeting* **2007**, *15*, 465.
(27) Ayman, E.-F.; Fernando, A. *J. Pept. Sci.* **2010**, *16*, 6.
(28) Inouye, K.; Voynick, I. M.; Delpierre, G. R.; Fruton, J. S. *Biochemistry* **1966**, *5*, 2473.
(29) Ulijn, R. V. *J. Mater. Chem.* **2006**, *16*, 2217.
(30) Sperinde, J. J.; Griffith, L. G. *Macromolecules* **2000**, *33*, 5476.
(31) Mann, B. K.; Gobin, A. S.; Tsai, A. T.; Schmedlen, R. H.; West, J. L. *Biomaterials* **2001**, *22*, 3045.
(32) West, J. L.; Hubbell, J. A. *Macromolecules* **1998**, *32*, 241.
(33) Broyer, R. M.; Quaker, G. M.; Maynard, H. D. *J. Am. Chem. Soc.* **2007**, *130*, 1041.
(34) Reynhout, I. C.; Lowik, D. W. P. M.; Hest, J. C. M. v.; Cornelissen, J. J. L. M.; Nolte, R. J. M. *Chem. Commun.* **2005**, 602.
(35) Weiss, C.; Landfester, K. *Adv. Polym. Sci.* **2010**, *229*, 1.
(36) Rossmanith, R.; Weiss, C. K.; Geserick, J.; Hüsing, N.; Hörmann, U.; Kaiser, U.; Landfester, K. *Chem. Mater.* **2008**, *20*, 5768.

(37) Schiller, R.; Weiss, C. K.; Geserick, J.; Hüsing, N.; Landfester, K. *Chem. Mater.* **2009**, *21*, 5088.
(38) Schiller, R.; Weiss, C. K.; Landfester, K. *Nanotechnology* **2010**, *21*, 405603.
(39) Glangchai, L. C.; Caldorera-Moore, M.; Shi, L.; Roy, K. *J. Controlled Release* **2008**, *125*, 263.
(40) Landfester, K. *Angew. Chem., Int. Ed.* **2009**, *48*, 4488.
(41) Förster, T. *Naturwissenschaften* **1946**, *33*, 166.
(42) Stryer, L. *Annu. Rev. Biochem.* **1978**, *47*, 819.
(43) Knight, C. G.; Willenbrock, F.; Murphy, G. *FEBS Lett.* **1992**, *296*, 263.
(44) Brandrup, J.; Immergut, E. H.; Grulke, E. A. *Polymer Handbook*; 4th ed.; Wiley-Interscience: Hoboken, NJ, 1999; Vol. 1.
(45) Papsuevich, O. S.; Chipens, G. I.; Bakharev, V. D.; Petrova, T. A. *Pharm. Chem. J.* **1985**, *19*, 24.
(46) Bech, L. M.; Soerensen, S. B.; Breddam, K. *Biochemistry* **1993**, *32*, 2845.
(47) Kuhn, R.; Geider, K. *Chem. Ber.* **1968**, *101*, 3587.
(48) Lauer-Fields, J. L.; Broder, T.; Sritharan, T.; Chung, L.; Nagase, H.; Fields, G. B. *Biochemistry* **2001**, *40*, 5795.
(49) Turner, D. C.; Testoff, M. A.; Conrad, D. W.; Gaber, B. P. *Langmuir* **1997**, *13*, 4855.
(50) Yi, H.; Wu, L.-Q.; Bentley, W. E.; Ghodssi, R.; Rubloff, G. W.; Culver, J. N.; Payne, G. F. *Biomacromolecules* **2005**, *6*, 2881.
(51) Hyun, J.; Kim, J.; Craig, S. L.; Chilkoti, A. *J. Am. Chem. Soc.* **2004**, *126*, 4770.
(52) Crespy, D.; Landfester, K. *Macromolecules* **2005**, *38*, 6882.
(53) Crespy, D.; Stark, M.; Hoffmann-Richter, C.; Ziener, U.; Landfester, K. *Macromolecules* **2007**, *40*, 3122.
(54) Crespy, D.; Landfester, K. *Polymer* **2009**, *50*, 1616.
(55) Aschenbrenner, E. M.; Weiss, C. K.; Landfester, K. *Chem.—Eur. J.* **2009**, *15*, 2434.
(56) Stupishina, E.; Khamidullin, R.; Vylegzhanina, N.; Faizullin, D.; Zuev, Y. *Biochemistry (Moscow)* **2006**, *71*, 533.
(57) Gessner, A.; Lieske, A.; Paulke, B.-R.; Müller, R. H. *J. Biomed. Mater. Res., Part A* **2003**, *65A*, 319.
(58) Blunk, T.; Hochstrasser, D. F.; Sanchez, J.-C.; Müller, B. W.; Müller, R. H. *Electrophoresis* **1993**, *14*, 1382.
(59) Schlaad, H.; Kukula, H.; Rudloff, J.; Below, I. *Macromolecules* **2001**, *34*, 4302.